Research Journal of Applied Sciences, Engineering and Technology 7(23): 5072-5081, 2014
DOI:10.19026/rjaset.7.902
ISSN: 2040-7459; e-ISSN: 2040-7467

Submitted: March 13, 2014 Accepted: April 11, 2014 Published: June 20, 2014

Research Article

Fluoresence Image Denoising using Diverese Strategies and their Performance Evaluation

[1]K. Sampath Kumar and [2]C. Arun
[1]Department of Electronics and Communication Engineering, Sree Sastha College of Engineering,
[2]Department of Electronics and Communication Engineering, R.M.K. College of Engineering and Technology, St. Peters University, Chennai, India

Abstract: Low illumination environment in Fluorescence microscopy, create arbitrary variations in the photon emission and detection process that manifest as Poisson noise in the captured images. Therefore study the effect of Standard denoising algorithms wherein the noise is either transformed to Gaussian or the denoising is done on the Poisson noise itself. In the first strategy the noise is Gaussianized by applying the Anscombe root transformation to the data, to produce a signal in which the noise can be treated as additive Gaussian and then the consequential image is denoised using conservative denoising algorithms for additive white Gaussian noise such as BLS_GSM and OWT_SURELET and finally the inverse transformation is done on the denoised image. The choice of the proper inverse transformation is vital for fluorescence images in order to reduce the bias error which arises when the nonlinear forward transformation is applied. The Latter strategy considers PURELET technique where the denoising process is a Linear Expansion of Thresholds (LET) that optimize results by depending on a purely data-adaptive unbiased estimate of the Mean-Squared Error (MSE), derived in a non-Bayesian framework (PURE: Poisson-Gaussian unbiased risk estimate). Experimental results are compared with exisitng work on how the ISNR changes with the change in algorithms for fluorescence images.

Keywords: Anscombe transformation, fluorescence, mixed-poisson-gaussian, poisson-gaussian unbiased risk estimate

INTRODUCTION

Fluorescence microscopy is a popular live imaging practice, used to image biological specimens. This technique has rigid constraints for parameters like acquisition-time and photo toxicity. Low illumination conditions generate arbitrary variations in the photon emission and detection process that manifest as Poisson noise in the captured images (Sampath and Arun, 2012). Successful denoising algorithms are consequently indispensable before visualization and analysis of these images.

In this study main aim of the work is to establish the impact of various standards denoising strategies on fluorescence images (Sampath and Arun, 2013). Photon and camera readout noises in general degrade fluorescence images. Thus the stochastic data representation is a Mixed-Poisson-Gaussian (MPG) procedure. Therefore consider strategies which moreover work on the Poisson noise or Gaussianize the Poisson process and then denoise the Gaussianized image (Luisier *et al*., 2010).

For Gaussianizing the images were carriedout to Variance Stabilizing Transform (VST) and applied to Anscombe root transformation $f: z \rightarrow 2\sqrt{z+\frac{3}{8}}$ to the data which determination of Gaussianize the noise which is then removed using a conventional denoising algorithm for additive white Gaussian noise ,which in our case is OWT_SURELET and BLS_GSM algorithms. An inverse transformation is used to estimate the signal of interest for denoised signal.

Proper inverse transformation is primary in order to reduce the bias error which prone position when the nonlinear forward transformation is performed (Fryzlewicz and Nason, 2004). Anscombe (1948) developed an algebraic inverse and the asymptotically unbiased inverse that together show the way to a substantial bias at low counts.

In this study also study the result of the PURELET algorithm whereas PURE algorithm unbiased results are estimated by using Haar wavelet domain, of the mean-squared error among the original image and the estimated image (Portilla *et al*., 2003). PURE-LET estimates the original image from the noisy image by estimation of PURE results with less MSE.

Corresponding Author: K. Sampath Kumar, Department of Electronics and Communication Engineering, Sree Sastha College of Engineering, St. Peters University, Chennai, India

THEORY

Poisson noise: Image acquisition step observes the original pixel values and it is defined as z_i, i = 1,… …, N. Where each and every z_i to be an self-determining random Poisson variable whose mean $y_i \geq 0$ is the fundamental intensity value to be estimated (Kolaczyk and Dixon, 2000). Clearly, the discrete Poisson probability of each z_i is:

$$E\{zi|yi\} = \frac{\mathrm{yi}^{\mathrm{zi}} e^{-yi}}{\mathrm{zi!}} \quad (1)$$

The mean Poisson variable z_i and variance of parameter y_i is defined as follow:

$$E\{zi|yi\} = yi = var\{zi|yi\} \quad (2)$$

Poisson noise can be formally defined as:

$$\eta i = zi - E\{zi|yi\} \quad (3)$$

Thus, trivially have $E\{\eta i|yi\} = 0$ and $var\{\eta i|yi\} = var\{zi|yi\} = yi$. Because possion noise variance results purely depends on the result of original intensity value. More purposely, the standard deviation of the noise ηi equals$\sqrt{yi}$. Outstanding the result of Poisson noise increases accordingly the signal-to-noise ratio decreases as the intensity value decreases (Willett and Nowak, 2003; Willett, 2006).

Variance stabilization and the Anscombe transformation: The rationale following for applying a variance-stabilizing transformation is to eliminate noise variance from data dependence, thus it becomes constant throughout the whole data $zi, i = 1, \ldots\ldots, N$. Moreover if the variance-stabilizing transformation is performed and then next predictable denoising method was designed for estimation of intensity values with a white Gaussian noise (Anscombe, 1948; Portilla *et al*., 2003). Exact stabilization or exact normalization based methods are possible to estimate the result of asymptotical. One of the important methods to analysis the result of asymptotical using variance-stabilizing transformations is the Anscombe transformation (Bo *et al*., 2008):

$$f: z \to 2\sqrt{z + \frac{3}{8}} \quad (4)$$

Applying Eq. (4) results the asymptotically additive standard normal noise with Poisson distributed data. The denoising signal of $f(z)$ produces a signal D which is measured as an estimation of $E\{f(z)|y\}$.

Denoising:

- Gaussian Denoisin
- Gaussian Denoising-BLS-GSM

Gaussian denoising BLS-GSM method is based on a numerical model of the coefficients and is used for removing noise data from digital images. In this statically model the coefficient of Neighborhoods at neighboring positions and their corresponding scales are modeled by making combination of two independent arbitrary variables that is a Gaussian vector and a hidden positive scalar multiplier. In this model each and every coefficient of Neighborhoods error values are estimated using Bayesian least square estimation in Eq. (8) and thus decreases the weighted average values of the local linear, it evaluates the overall probable result of hidden multiplier variable. Top level structure based procedure followed for image denoising:

- Decompose the image into pyramid sub bands at diverse scales and orientations
- Denoise every subband, excluding for the low pass residual band
- Reverse the pyramid transform, achieving the result of denoised image

Phyramid representation of the vector y defines the values for neighborhood of observed coefficients x and it can be expressed as:

$$y = x + w = \sqrt{z}u + w \quad (5)$$

In the Eq. (4) coefficient of neighborhood together with the combination of three independent additives Gaussian noises shown in Eq. (5). Together u and w are zero-mean Gaussian vectors, with related covariance matrices Cu and Cw. The density of the experimental neighborhood coefficient vector y conditioned with a zero-mean Gaussian value, with covariance:

$$C(y|z) = zCu + Cw$$

$$p(y|z) = exp\left(\frac{\frac{-y^T(zCu+Cw)^{-1}y}{2}}{\sqrt{(2\pi)^N\,||zCu+Cw||}}\right) \quad (6)$$

The neighborhood noise covariance Cw, is obtained by decomposing a delta function $\sigma\sqrt{NyNx}\delta(n,m)$ into pyramid sub bands, where (Ny, Nx) are the image dimensions. Elements of Cw computed by using as sample covariance (Thierry and Florian, 2007). This procedure is simply widespread for nonwhite noise, by changing the delta function with the inverse Fourier transform by taking square root value for noise power spectral density. Known Cw values are computed from the observation covariance matrix Cy. Then calculate from $C(y|z)$ by taking expectations over z:

$$C(y) = E\{z\}Cu + Cw$$

Without loss of generality by setting $E\{z\} = 1$, resulting in:

$$Cu = Cy - Cw \quad (7)$$

Bayes least squares estimator: For every neighborhood least square estimation first need to calculate the reference coefficient x_c, that is closer to middle neighborhood coefficient observed from set of noisy coefficients. The Bayes least squares (BLS) estimate is just the conditional mean:

$$\begin{aligned} E\{x_c|y\} &= \int x_c p(x_c|y)\, dx_c \\ &= \int \int_0^\infty x_c p(x_c, z|y)\, dz dx_c \\ &= \int \int_0^\infty x_c p(x_c|y, z) p(z|y)\, dz dx_c \\ &= \int_0^\infty p(z|y)\, E\{x_c|y, z\} dz \end{aligned} \quad (8)$$

where, each has unspecified still convergence in order to swap the order of integration. Now describing the each of these individual components.

Local wiener estimate: The major advantage of this methods is that the coefficient of neighborhood vector x is conditioned with a zero-mean Gaussian value z. This information, coupled with the supposition of additive Gaussian noise in Eq. (8) basically a local linear (Wiener) estimate. Writing this for the full neighborhood vector:

$$E\{x|y, z\} = zC_u(zC_u + C_w)^{-1} y \quad (9)$$

Solving the above equation and now it is changed as:

$$E\{x_c|y, z\} = \sum_{n=1}^{N} \frac{z m_{cn} \lambda_n v_n}{z\lambda_n + 1} \quad (10)$$

Posterior distribution of the multiplier: The other module of the solution given in (8) is the distribution of the multiplier, conditioned on the observed neighborhood values and the probability $p(z|y)$ is calculated by using Bayes' rule is defined as below:

$$p(z|y) = \frac{p(y|z) p_z(z)}{\int_0^\infty p(y|\alpha) p_z(\alpha) d\alpha} \quad (11)$$

Summarizing our denoising algorithm:

1) Decompose the image into sub bands.
2) For each sub band excluding the low pass residual:
   a) Compute neighborhood noise covariance, C_w, from the image-domain noise covariance C_v.
   b) Estimate noisy neighborhood covariance, C_y
   c) Estimate C_u from C_w and C_y using (7).
   d) Compute Λ and M
   e) For each neighborhood:
   f) For each value z in the integration range:
   g) Compute $E\{x_c|y, z\}$ using (10).
   h) Compute $p(y|z)$
   i) Compute$p(z|y)$ using (11)
   j) Compute $E\{x_c|y, \}$ numerically using (8)
3) Reconstruct the denoised image from the processed sub bands and the low pass residual to get original image D.

Gaussian denoising OWT_SURELET: In SURE, no *a priori* image representation is desired to optimize the denoising procedure, which then purely amounts to solving a linear scheme of equations in every wavelet sub band. General denoising approach includes the denoising expression of F(y), with linear expansion of threshold for known basic processes, $F_k(y)$:

$$F(y) = \sum_{k=1}^{K} akFk(y) \quad (12)$$

Here, the unknown weights ak are precised by minimization of SURE error values the SURE. It is also probable to measure the performance of proposed work and compare experimental result with MSE.

The linearity of the expansion (12) is a critical benefit for solving the minimization problem MSE, since the SURE is quadratic in $F(y)$.The coefficients ak are, thus, the explanation of a linear system of equations:

$$\begin{aligned} &\frac{\sum_{t=1}^{K} Fk(y)^T Ft(y)}{[M]k,l} = \frac{Fk(y)^T y - \sigma^2 div\{Fk(y)\}}{[c]k} \\ &\text{For k = 1, 2, … K} \\ &\text{Ma = c} \end{aligned} \quad (13)$$

These approaches suggest choosing a group of different denoising algorithms preferably with balancing denoising behaviors and optimizing a weighting of these algorithms to obtain the greatest of them at once.

In the remainder of this study, would focus on a point wise thresholding as an alternative of a specific algorithm.

Point wise SURE-LET transform denoising: First describe a pair of linear transformations D-decomposition and R-reconstruction such that RD = Identity: usually D is a bank of decimated or undecimated filters. Once the size of the input and output data are frozen, these linear operators are characterized by matrices, respectively $D = (di, j)_{i,j\in[1:L]\times[1:N]}$ and $R = (ri, j)_{i,j\in[1:L]\times[1:N]}$ that satisfy the perfect reconstruction property $RD = ID$. Then, the entire denoising procedure boils down to the following steps.

- Apply D to the noisy signal $y = x + b$to get the transformed noisy coefficients$w = Dy = (wi)_{i\in[1:L]}$.
- Apply a point wise thresholding function $(\theta i(wi))_{i\epsilon[1:L]}$
- Revert to the original domain by applying R to the thresholded coefficients$\theta(w)$, yielding the denoised estimate$\widehat{x}$ = R $\theta(w)$.

This algorithm can be summarized as a function of the noisy input coefficients:

$$\widehat{x} = \mathrm{F(y)} = \mathrm{R}\,\theta(Dy) \quad (14)$$

Expressing F as a linear expansion of denoising algorithms Fk, SURE-LET approch suggests the following equation:

$$\frac{F(y)=\sum_{k=1}^{K} akR\theta k(Dy)}{\mathrm{Fk(y)}} \quad (15)$$

where, $\theta k(.)$ are basic point wise thresholding functions. This linear parameterization doesn't depend on a linear denoising; definitely, the thresholding functions can be selected as nonlinear.

A point wise thresholding function is possible to be well-organized if it satisfies the following properties such as Differentiability, Anti-symmetry and Linear behavior for large coefficients. A good selection has been experimentally found to be of the type of:

$$\theta i(w)$$
$$\theta i(w) = ai, 1t1(w) + ai, 2t2(w)$$

where,

$$t1(w) = w \text{ and } t2(w) = w(1 - e^{-(\frac{w}{3\sigma})^8}) \quad (16)$$

in each band i.

Summary of the algorithm:

1) Perform a boundary extension on the noisy image.
2) Perform an UWT on the extended noisy image.
3) For i = 1….J (number of band pass subbands), For k = 1, 2:

a. Apply the efficient point wise thresholding functions defined in (16) to the current subband wi.
b. Reconstruct the processed subband by setting all the other subbands to zero to achieve Fi,k(y).
c. Calculate the first derivative of tk for every coefficient of the current sub band wi and costruct the equivalent coordinate of c as exemplified by (13).

end.
end.

Poisson denoising:

Poisson denoising PURELET: The basic theory behind this is to find a statistical approximation of the Mean Square Error (MSE) among unknown noiseless image and the known noisy image. Due to the Poisson noise theory referring the result of outcomes using PURE; it is compared to Stein's Unbiased Risk Estimate (SURE) which holds for Gaussian information.

The main aim of this study is to minimize the MSE to estimate the denoising result to discover the greatest one, in the sense of the Signal-to-Noise Ratio (SNR), which is a widespread quantifier of restoration quality. The effectiveness of the method stems beginning the use of a straightforward normalized Haar-wavelet transform and from the perception of Linear Expansion of Thresholds (LET) because the weight values are unknown.

These weight values are calculated by minimizing the PURE, throughout the resolution of an easy linear system of equations. Since every one of the parameters in algorithm is adjusted completely by design, without any need of user. For each sub band, our restoration functions consist of several parameters with more flexibility than normal single-parameter thresholding functions. Significantly, the thresholds are modified to local estimates of the noise variance.

Correspondingly our proposed schema for SURE-based denoising method defines the thersholding parameter with linear expansion of thresholds (LET) defined as:

$$\mathrm{F(y)} = \sum_{\mathrm{k=1}}^{\mathrm{K}} \mathrm{akR\Theta k(w, \bar{w})}$$

where,

$$\mathrm{R\Theta k\,(w, \bar{w}) = Fk(y)} \quad (17)$$

It becomes more efficient than normal PURE becomes quadratic in theak's. Consequently, the search for the best vector of parameters $\mathrm{a} = [\mathrm{a1, a2 \ldots ak}]^{\mathrm{T}}$ boils down to the result of the follow system of linear equations:

for k = 1..K:

$$\frac{\sum_{l=1}^{K} fk(y)^T fl(y)a}{[M]k,l} = \frac{(y)^T \bar{f_k}(y) - \sigma^2 div\{\bar{f_k}(y)\}}{[c]k}$$

For k = 1, 2, …K

$$\mathrm{Ma = c} \quad (18)$$

While using the first-order Taylor-series approximation of PURE then obtain an equivalent system of linear equations given by:

$$\hat{c} = [y^T(f_k(y) - \partial f_k(y)) - \sigma^2 div\{f_k(y) - \partial fky] \; k \in 1 \ldots K \quad (19)$$

Inverse transformation: Inverse transformation function is applied to estimate the desired value of y. The direct algebraic inverse of (4) is:

$$Ia(D) = f^{-1}(D) = \left(\frac{D}{2}\right)^2 - \frac{3}{8} \quad (20)$$

But the substantial estimate of y is biased, since the nonlinearity of the transformation f means generally have:

$$E\{f(z)|y\} \neq f(E\{z|y\}). \quad (21)$$

And, thus:

$$f^{-1}(E\{f(z)|y\}) \neq E\{z|y\} \quad (22)$$

Another possibility is to use the adjusted inverse:

$$Ib(D) = \left(\frac{D}{2}\right)^2 - \frac{1}{8} \quad (23)$$

This provides asymptotical unbiasedness for maximum counts. This is the inverse characteristically used in applications.

While the asymptotically unbiased inverse (22) results provides efficient for high-count data, applying it to low-count data leads to a biased estimate.

Exact unbiased inverse: Provided a well efficient denoising, i.e., D is treated as $E\{f(z)|y\}$, the accurate unbiased inverse of the Anscombe transformation, f is an inverse transformation that maps the values $E\{f(z)|y\}$ to the desired values $E\{z|y\}$:

$$Ic: E\{f(z)|y\} \rightarrow E\{z|y\} \quad (24)$$

Because $E\{z|y\} = y$ for any given y, the hitch of finding the inverse Ic reduces to calculating the values of $E\{f(z)|y\}$, it is done by using arithmetical calculation of the integral equivalent to the expectation operator E:

$$E\{f(z)|y\} = \int_{-\infty}^{\infty} f(z)p(z|y)\,dz \quad (25)$$

where, $p(z|y)$ is the generalized conditional probability density function of z on y. In this study use discrete Poisson probabilities $p(z|y)$ so it can be replcae the integral part by summation:

$$E\{f(z)|y\} = \sum_{z=0}^{\infty} f(z)p(z|y) \quad (26)$$

Further, because here $f(z)$ is the forward Anscombe transformation then rewrite the above (25) equation as:

$$E\{f(z)|y\} = 2\sum_{z=0}^{\infty}\left(\sqrt{z+\frac{3}{8}}.\frac{y^z e^{-y}}{z!}\right) \quad (27)$$

Let us refer to that if the exact unbiased inverse value in (23) and it is directly applied to the denoised data D with a little error and then the estimation error $\hat{y} = Ic(D)$ can contain variance as well as bias components. In common, the unbiasedness of Ic holds simply provided that $D = E\{f(z)|y\}$ accurately, as it is unspecified.

EXPERIMENTS

All of our experiments consist of the both Gaussian based denoising strategies and Poisson based denoising strategy. Gaussian based denoising approach constitutes of the same three-step denoising forward Anscombe transformation (4) procedure to a noisy image after which denoising of the transformed image with OWT_SURELET (Thierry and Florian, 2007) BLS_GSM (Portilla *et al*., 2003) and finally apply an inverse transformation in order to get the final estimate. To apply the accurate unbiased inverse Ic, it is adequate to compute (26) for a restricted set of values y; for random values of y computed using linear interpolation values from (26) and for large values of y approximate Ic by Ib. It is also calculate the PURELET strategy for the equal images. The performances of these algorithms are evaluated by the peak signal-to-noise ratio (PSNR). The PSNR is calculated using the formula:

$$10\log_{10}\left(\frac{max(yi)^2}{\sum_i((\hat{y}i-yi)^2|N)}\right) \quad (28)$$

where, N is the total number of pixels in the image.

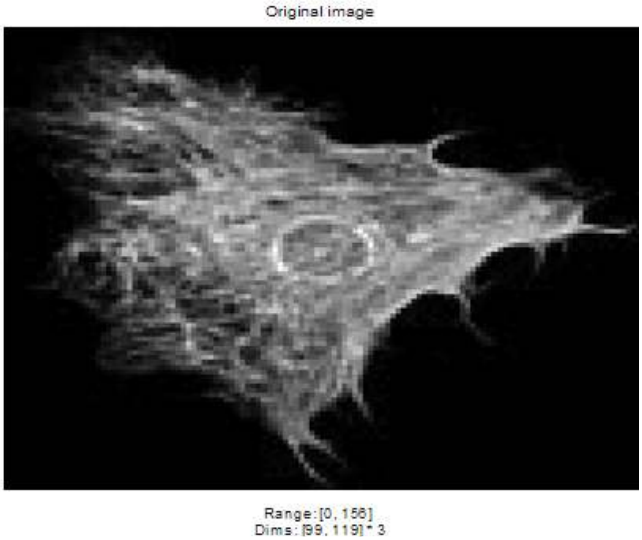

Fig. 1a: Lung tissue of an adult female grey fox

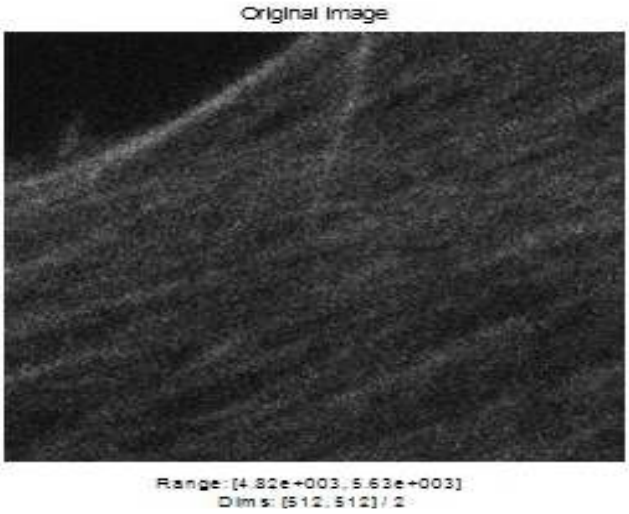

Fig. 1b: Image of Phalloidin staining

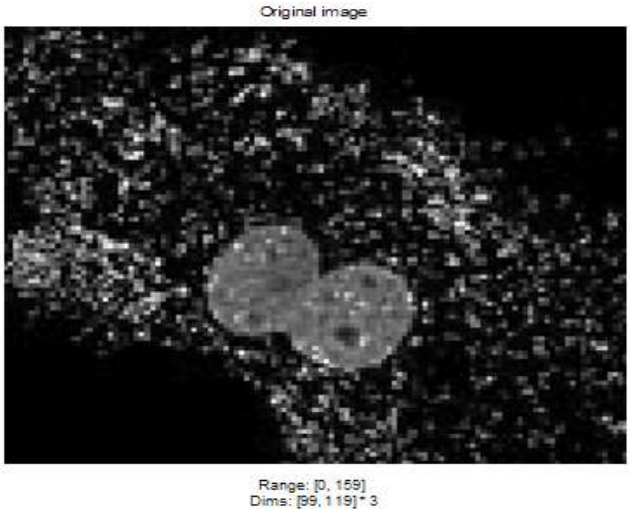

Fig. 1c: Embryonic Albino Swiss mouse fibroblast cells

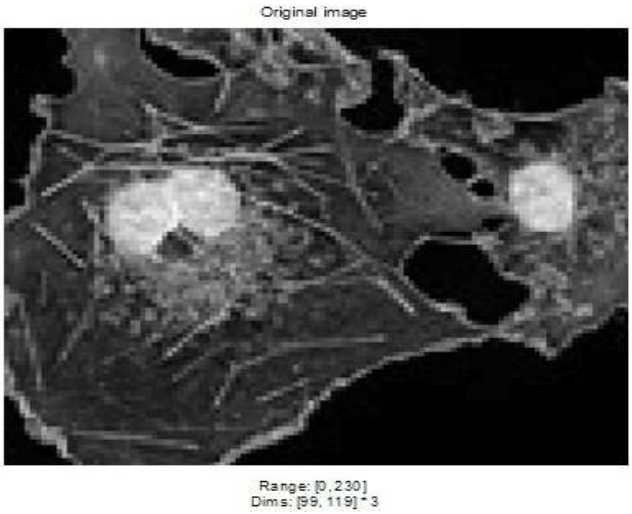

Fig. 1d: Transformed African green monkey kidney F broblast cells

Table 1: Test results using Bls-Gsm

	Figure 1a		Figure 1b		Figure 1c		Figure 1d	
Images σ	ISNR With Asymptotic Inverse	ISNR with exact unbiased inverse	ISNR with asymptotic inverse	ISNR with exact unbiased inverse	ISNR with asymptotic inverse	ISNR with exact unbiased inverse	ISNR with asymptotic inverse	ISNR with exact unbiased inverse
1	18.3733	18.3788	37.928	37.928	20.8926	20.9045	21.0092	21.0103
2	12.3533	12.3547	37.7762	37.7762	10.0408	10.0415	13.8841	13.8842
5	8.7174	8.718	37.4882	37.4882	2.1305	2.1306	8.4743	8.4743
10	6.3147	6.315	37.2215	37.2215	0.86797	0.86805	6.332	6.332
15	4.8577	4.8579	37.011	37.011	-0.01025	-0.010188	5.2478	5.2478
20	3.3614	3.3615	36.8504	36.8504	-1.052	-1.052	4.4453	4.4453
25	1.9348	1.9349	36.6522	36.6522	-2.1395	-2.1395	3.5624	3.5624

Table 2: Test results using Owt-Surelet

	Figure 1a		Figure 1b		Figure 1c		Figure 1d	
Images σ	ISNR with asymptotic inverse	ISNR with exact unbiased inverse	ISNR with asymptotic inverse	ISNR with exact unbiased inverse	ISNR with asymptotic inverse	ISNR with exact unbiased inverse	ISNR with asymptotic inverse	ISNR with exact unbiased inverse
1	20.7809	20.7809	33.2325	33.2325	32.2628	32.2628	46.2268	46.2268
2	7.2921	7.2921	21.1491	21.1491	21.8615	21.8615	41.1083	41.1083
5	-19.8475	-19.8475	2.4624	2.4624	-0.7134	-0.7134	33.7373	33.7373
10	-42.3704	-42.3704	-18.3072	-18.3072	-21.2937	-21.2937	27.9214	27.9214
15	-55.5672	-55.5672	-32.1022	-32.1022	-34.4599	-34.4599	24.4688	24.4688
20	-64.9806	-64.9806	-42.3147	-42.3147	-44.0059	-44.0059	22.0049	22.0049
25	-71.9272	-71.9272	-50.4210	-50.4210	-51.4470	-51.4570	20.0877	20.0877

Table 3: Test results using pure-let

Images	Figure 1a	Figure 1b	Figure 1c	Figure 1d
Σ	UWT PURELET	UWT PURELET	UWT PURELET	UWT PURELET
1	36.6208	33.9654	43.3324	36.1422
2	35.6699	33.3647	40.2298	35.2649
5	32.1363	30.8332	33.7215	31.9019
10	27.4721	26.8765	27.9898	27.3493
15	24.2687	23.9201	24.5352	24.1935
20	21.8901	21.6546	22.0610	21.8401
25	12.9289	19.8365	20.1360	19.9752

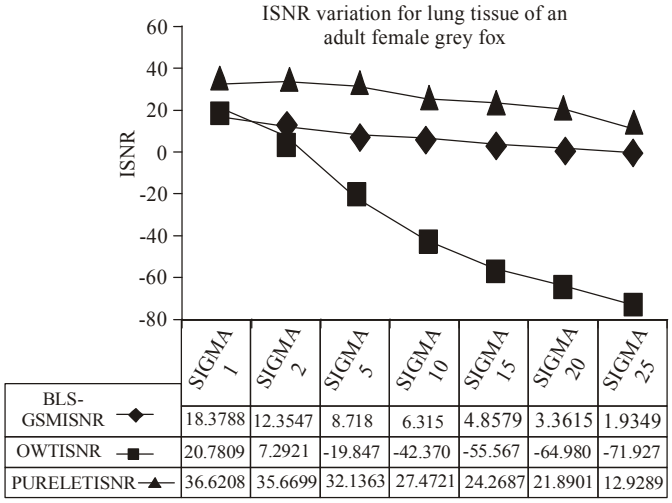

(a)

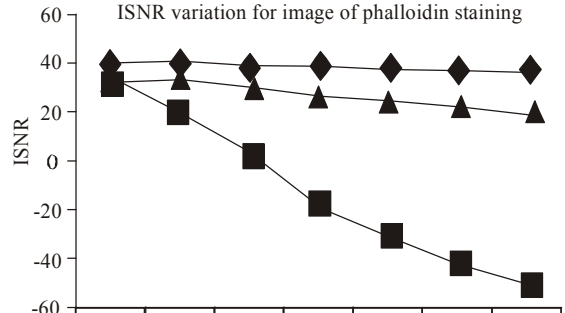

	SIGMA 1	SIGMA 2	SIGMA 5	SIGMA 10	SIGMA 15	SIGMA 20	SIGMA 25
BLS-GSMISNR	37.928	37.7762	37.4882	37.2215	37.011	36.8504	36.6522
OWTISNR	33.2325	21.1491	2.4624	-18.307	-32.102	-42.314	-50.421
PURELETISNR	33.9654	33.3647	30.8332	26.8765	23.9201	21.6546	19.8365

(b)

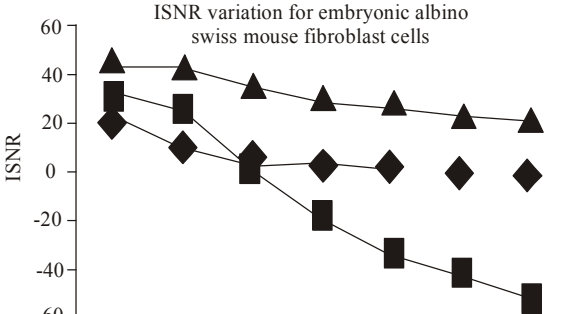

	SIGMA 1	SIGMA 2	SIGMA 5	SIGMA 10	SIGMA 15	SIGMA 20	SIGMA 25
BLS-GSMISNR	20.9045	10.0415	2.1306	0.86805	-0.0101	-1.052	-2.1395
OWTISNR	32.2628	21.8615	-0.7134	-21.293	-34.459	-44.005	-51.447
PURELETISNR	43.3324	40.2298	33.7215	27.9898	24.5352	22.061	20.136

(c)

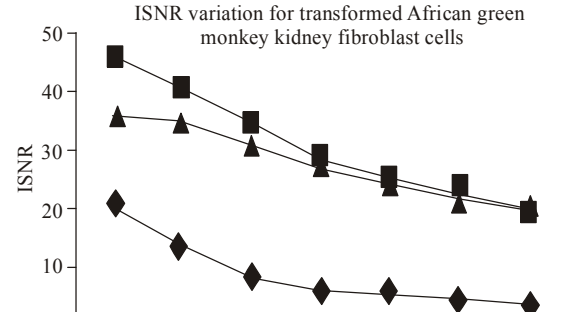

	SIGMA 1	SIGMA 2	SIGMA 5	SIGMA 10	SIGMA 15	SIGMA 20	SIGMA 25
BLS-GSMISNR	21.0103	13.8842	8.4743	6.332	5.2478	4.4453	3.5624
OWTISNR	46.2268	41.1083	-33.7373	-27.9214	24.4688	22.0049	20.0877
PURELETISNR	36.1422	35.2649	31.9019	27.3493	24.1935	21.8401	19.9752

(d)

Fig. 2: Comparison of various denoising algorithms with respect to sigma

In our experiments using the test images was shown in Fig. 1a to c and evaluates the performance in terms of PSNR. Using OWT-SURELET, BLS_GSM and PURELET for the denoising and the inversion is done with either the exact unbiased inverse or the asymptotically unbiased inverse.

The denoising performance is evaluated in terms of PSNR and compares the results obtained with the results obtained in Sampath and Arun (2012, 2013). Table 1 present the results in Sampath and Arun (2012). Table 2 shows the in Sampath and Arun (2012) and Table 3 shows the results of PURELET. The plots of the PSNR values obtained using BLS_GSM, OWT SURELET and PURELET at a glance shows that PURELET outperforms the other two strategies in general for fluorescence image.

RESULTS

The four test images used in the experiment (Fig. 1). Plots of results (Fig. 2); Plots of results (Fig. 3 and 4).

CONCLUSION

Results from PURE-LET denoising shows great improvement in the ISNR value when compared to OWT SURELET denoising and BLS_GSM denoising strategies. Generally PURE-LET strategy out beats OWT_SURELET and BLS_GSM strategy, but shows a reduction in ISNR when compared to BLS_GSM only for low count image. A comparative study of BLS_GSM and OWT-SURELET strategies show that OWT provides higher ISNR when the sigma value is low. As the sigma value increases there is a steep fall in the signal to noise ratio. The BLS_GSM showed improvement when using the exact unbiased transform for low count images. Whereas for OWT-SURELET both asymptotic inverse transform and exact unbiased inverse transform produced the same results. The total comparison of results shows that the PURELET strategy is the better choice for fluorescence images and outperforms BLS_GSM and OWT_SURELET.

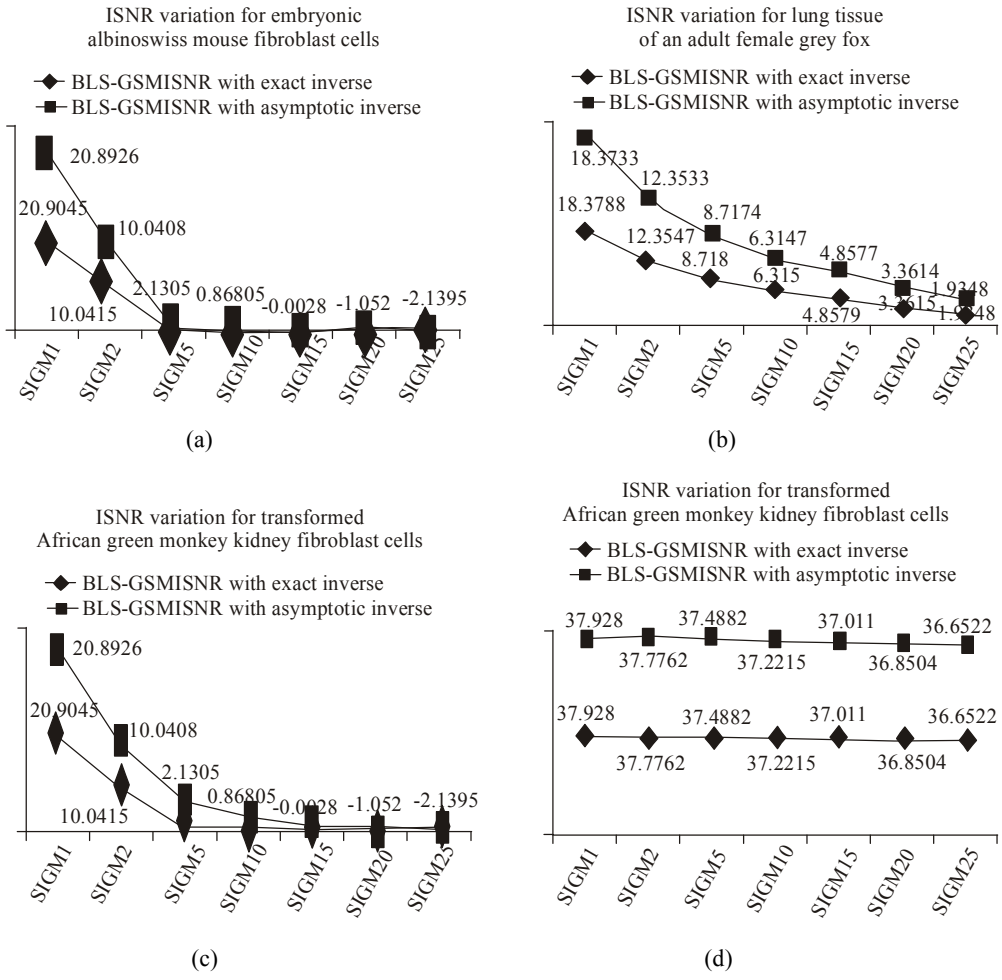

Fig. 3: Comparison of exact and asymptotic inverse transforms using BLS_GSM

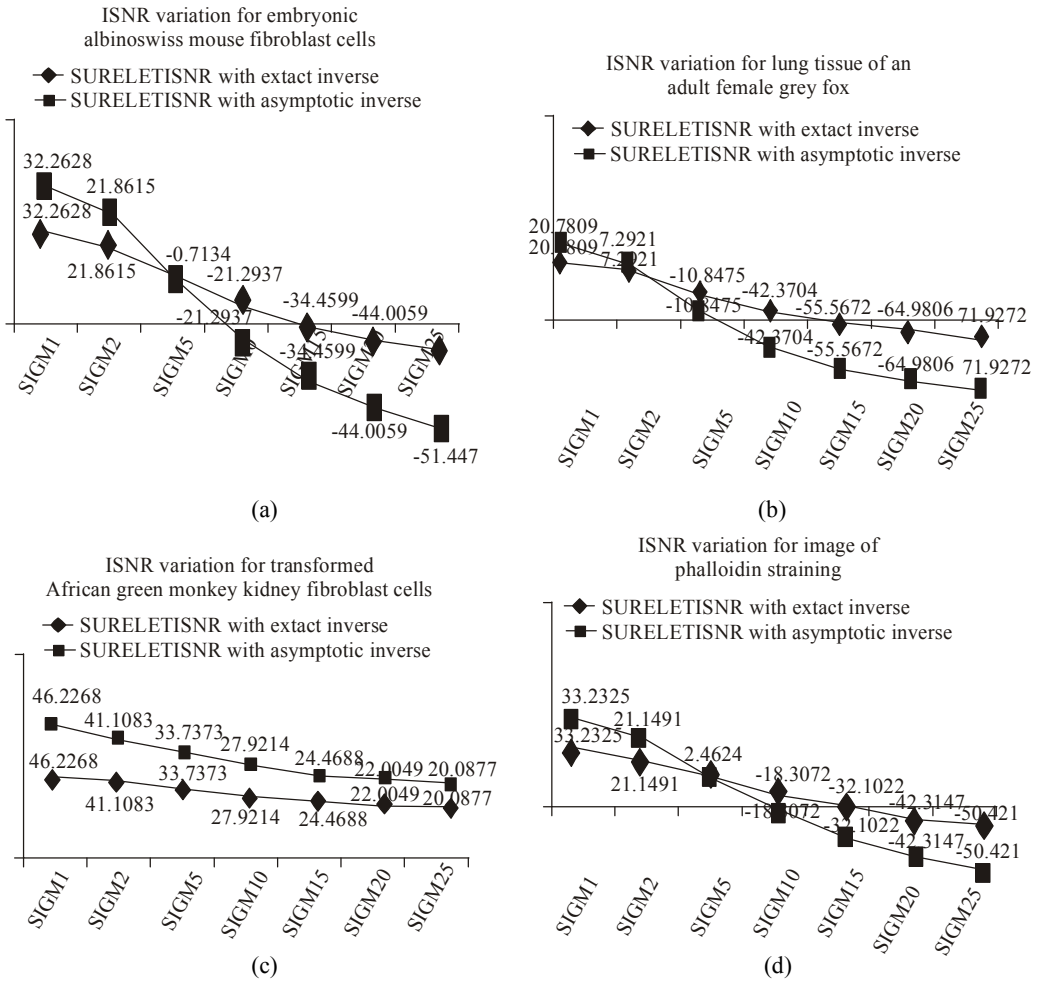

Fig. 4: Comparison of exact and asymptotic inverse transforms using OWT-SURELET

REFERENCES

Anscombe, F.J., 1948. The transformation of Poisson, binomial and negative binomial data. Biometrika, 35(3/4): 246-254.

Bo, Z., M.F. Jalal and S. Jean-Luc, 2008. Wavelets, ridgelets and curvelets for poisson noise removal. IEEE T. Image Process., 17(7).

Fryzlewicz, P. and G.P. Nason, 2004. A haar-fisz algorithm for poisson intensity estimation. J. Comput. Graph. Stat., 13(3): 621-638.

Kolaczyk, E.D. and D.D. Dixon, 2000. Nonparametric estimation of intensity maps using Haar wavelets and Poisson noise characteristics. Astrophys. J., 534(1): 490-505.

Luisier, F., C. Vonesch, T. Blu and M. Unser, 2010. Fast inter scale wavelet denoising of poisson-corrupted images. Signal Process., 90(2): 415-427.

Portilla, J., V. Strela, M.J. Wainwright and E.P. Simoncelli, 2003. Image denoising using scale mixtures of Gaussians in the wavelet domain. IEEE T. Image Process., 12(11): 1338-1351.

Sampath, K. and C. Arun, 2012. Poisson Noise removal from fluorescence images using optimized variance-stabilizing transformations and standard Gaussian denoising strategies. Eur. J. Sci. Res., 84(3): 336-344.

Sampath, K. and C. Arun, 2013. An improved image denoising approach using optimized variance-stabilizing transformations. Int. Rev. Comput. Softw., 8(8): 1991-1996.

Thierry, B. and L. Florian, 2007. The SURE-LET approach to image denoising. IEEE T. Image Process., 16(11).

Willett, R.M., 2006. Multiscale analysis of photon-limited astronomical images. Proceeding of the 4th Conference on Statistical Challenges in Modern Astronomy (SCMA, 2006). State College, June 12th-15th.

Willett, R.M. and R.D. Nowak, 2003. Platelets: A multiscale approach for recovering edges and surfaces in photon-limited medical imaging. IEEE T. Med. Imaging, 22(3): 332-350.